A Highly Fluorinated Epoxy Resin. III. Behavior in Composite and Fiber-Coating Applications

T. E. TWARDOWSKI and P. H. GEIL*

Polymer Division, Department of Materials Science and Engineering,
University of Illinois, 1304 W. Green St., Urbana, Illinois 61801

SYNOPSIS

The behavior of a highly fluorinated epoxy resin used as a composite matrix material with AS-4 fibers and as an AS-4 fiber coating was studied. The composite mechanical properties were obtained, and the adhesion of the matrix to the fibers was evaluated. Comparisons of uncoated and fluoropolymer coated AS-4 fibers using single fibers embedded in an Epon 828 matrix were made. Substantial improvement in fiber critical length, and therefore fiber-matrix adhesion, was observed.

INTRODUCTION

Fluoroepoxies with improved properties such as surface tension and friction coefficients[1] and low water uptake[2] have been synthesized by Griffith and Field.[3,4] In the first paper of this series, C8/1SA was studied as a model material for these resin systems.[5] In the second paper, an attempt was made to incorporate the advantageous properties of the fluorinated resin in blends with standard resins. Toward this end, a model blend of C8/1SA with Epon 828 was studied.[6] Another alternative use of the fluoroepoxies could be their application as carbon fiber composite matrices and fiber coatings. This alternative was investigated, again using C8/1SA as a model system. The mechanical properties and nature of failure of C8/1SA-AS4 composite are reported here. Results of single-fiber tests, conducted in the manner described by Drzal[7] and Bascom and Jensen[8] on uncoated and C8/1SA coated AS4 fibers in an Epon 828 (E828)/1SA matrix are also reported.

EXPERIMENTAL

In an attempt to produce samples more or less representative of the potential use of C8 as a matrix for composites, samples consisting of ca. 50% graphite fibers were prepared. AS4 fibers were laid unidirectionally by hand in silicone molds of a dog-bone shape, $2.5 \times 0.5 \times \frac{1}{8}$ in. (l × w × h) with 1.5 × 0.25 (l × w) in. gauge. Stoichiometric amounts of C8 resin and 1SA hardener were mixed at 56°C for 20 min, then poured into the mold. The sample was outgassed under vacuum for 20 min, cured at room temperature for 16 h (under N_2) and postcured for 3 h at 120°C. The C8/1SA resin "wet out" the fibers well. The aging histories of the samples were removed by heating at 120°C for $\frac{1}{2}$ h just prior to testing. These samples were then tested in tension using an Instron 1331. One sample, which failed to break in tension, was fractured in flexure. One of this pair of fracture surfaces was polished and ion etched for 20 min. The fluorinated resin component is very susceptible to ionization. A Lepel high-frequency generator was used to generate an air molecule plasma. The ionized air molecules bombarded the surface of the sample that was maintained on a liquid N_2 cooled cold stage, enhancing the morphology. Both surfaces were coated with Au—Pd and examined using an Hitachi S570 SEM. The etched sample was examined at a working distance of 13 mm, whereas the shear fracture surface was examined at the maximum attainable working distance of 30 mm to obtain greater depth of field.

Coated AS4 fibers were prepared by carefully gluing the carbon fibers across a wire rack. C8/1SA resin was mixed in stoichiometric proportions and mixed for 30 min at 60°C. The reacting mixture was then diluted 12 : 1 with acetone and poured over the

* To whom correspondence should be addressed.

Journal of Applied Polymer Science, Vol. 42, 1721–1726 (1991)
 CCC 0021-8995/91/061721-06$04.00

fibers. These fibers were dried under vacuum at 30°C. Coated and uncoated AS4 fibers were embedded in single-fiber tensile samples with E828/1SA matrices. The molds were in two pieces, consisting of a $\frac{1}{8}$ in. deep cavity dogbone (with the same length, width, and gauge characteristics described above) over which several fibers were carefully laid. These fibers were held in place with a $\frac{1}{4}$ in. deep hollow dogbone mold, open at the top to allow outgassing of the resin. Stoichiometric amounts of E828 and 1SA were mixed at 50°C for 20 min, poured into the molds, outgassed under vacuum for 20 min, and then cured at room temperature under N_2 for 16 h and postcured for 3 h at 120°C. After curing, excess material was mechanically removed for a total specimen thickness of $\frac{1}{4}$ in. (with the fiber in the middle) and the surfaces were polished optically smooth with 0.3 micron alumina powder. The aging of the specimens was removed by heating as described above. Each sample type was examined under tension on a tensile stage attached to a Reichert Zetopan optical microscope. The formation of the birefringence was recorded photographically. Tension was released, and the critical lengths of the broken fibers were measured using a combination of bright-field and birefringence patterns to locate breakpoints.

The single-fiber tension test requires a number of tests determined by the variation in fracture length to evaluate a statistically significant value for the critical length; that is, if a given fiber breaks into 20 identical lengths, fewer samples are required than if widely scattered lengths are observed. Approximately statistical values were obtained here.

RESULTS AND DISCUSSION

The mechanical properties of the C8/1SA-AS4 composite drawn parallel to the fiber axis are shown in Figure 1. The shape is somewhat unusual, initially concave upward followed by a change to more normal elastic behavior at 0.35% strain. The composite was impossible to break in tension. No matter what the circumstances, the material would fail, breaking up into many pieces in the grips, while the run proceeded. Thus, the upper point in the figure does not represent the ultimate failure strength of the composite. The concave initial behavior is attributed to the initial stress being supported by a reduced number of fibers, the number increasing as the fibers straighten. The initial modulus of 16×10^3 ksi is very close to the theoretical value (by rule of mixtures) of 16.6×10^3 ksi, suggesting that most of the fibers are straight to begin with.

Low-magnification scanning electron micrographs of the polished and etched surface [Fig. 2(a)] show the random distribution of the AS4 fibers and the matrix disruption characteristic of the fluoroepoxy when exposed to the ion-etching process. The higher magnification in Figure 2(b) indicates that even under these adverse conditions material can be found adhering to many of the fibers.

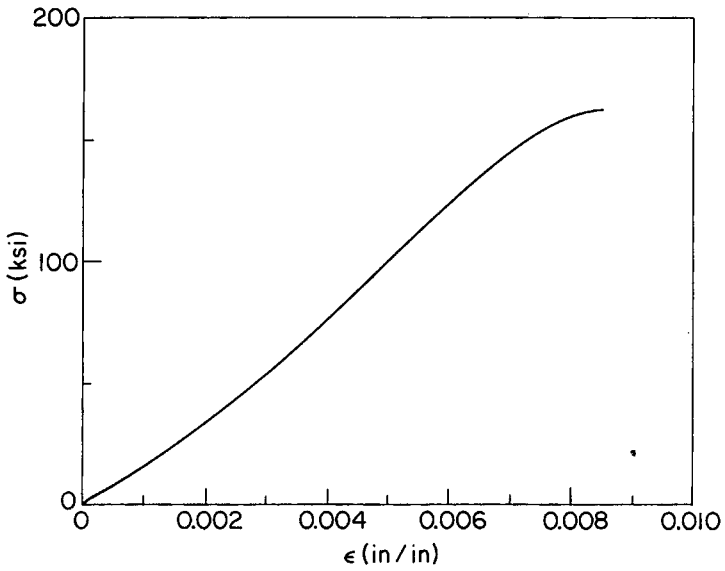

Figure 1 Stress-strain behavior of C8/1SA-AS4 unidirectional composite along fiber axis.

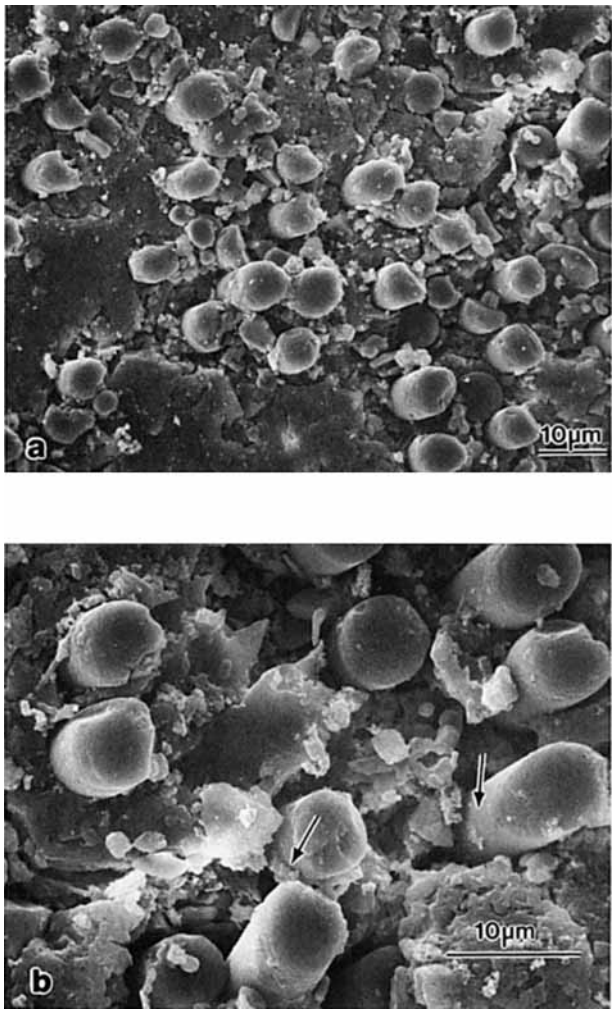

Figure 2 Micrographs of a composite flexurally fractured, surface polished, and ion etched for 20 min. (a) Low magnification showing fiber distribution. (b) Higher magnification: The arrow indicates regions where material is adhering to the fibers, despite the rigorous treatment.

Figures 3(a) and (b) are low- and high-magnification micrographs of the unetched flexure failure surface. In Figure 3(a), fibers can be seen to have been pulled from the matrix, whereas other fibers are protruding to such an extent that even at the largest working distance obtainable the ends are out of focus. For perfect adhesion, one would normally expect the fracture plane to proceed through the matrix and fibers along a path dictated by statistical failure of fibers. We note, however, that the fractured specimen had already undergone a tensile test. It is likely that during the tensile test the fibers fractured at points randomly throughout the gauge region and then debonded along the fibers due to interfacial shear, allowing the fibers to pull out as the fracture propagated during flexure. The arrow in Figure 3(b) points to a place where large quantities of fluoroepoxy are adhering to and binding two fibers together. This is usually taken as indicative of good adhesion.

The critical lengths of the two systems, Epon 828/1SA-AS4(C8/1SA), as determined in the single-fiber tests[7,8] are detailed in Table I. The critical length of the coated fibers is significantly smaller. Assuming the ultimate fiber strengths to be the same in both cases, this translates to a stronger interfacial strength.

In Figure 4, the development of the birefringence in a treated fiber sample as tension is applied is illustrated. Figure 4(a) shows the initial shape of the birefringence just as the initial breaks in the fiber are formed (indicated by the arrows). In Figure

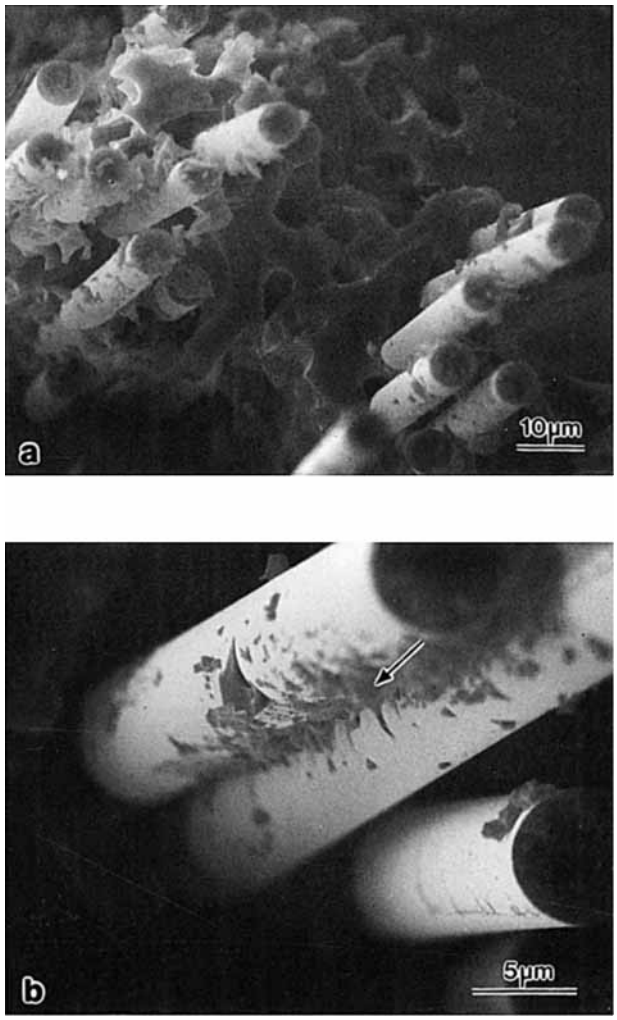

Figure 3 Micrographs of a composite flexurally fractured, surface unmodified. (a) Low magnification showing the fiber pullout. (b) Higher magnification: The arrow points to fluoroepoxy adhering to the fibers.

Table I Critical Lengths of Fibers in Single-fiber Tests

Matrix	Fiber	Critical Length
Epon 828/1SA	AS4	1.0 ± 0.4 mm
Epon 828/1SA	AS4/C8/1SA	0.5 ± 0.2 mm

4(b), the leftmost fiber break has moved out of the field to the left, while another break has occurred (indicated by the arrow slightly left of center). The birefringence pattern is also noted to begin to localize, becoming closer to the fiber. Drzal[9] has indicated that this could be due to the progress of fiber debonding or, in this case, to debonding of the matrix and fiber coating. On the other hand, the C8/1SA coating, in its nonaged state, is much more compliant than is the matrix, perhaps concentrating the strain in a narrow sheath close to the fiber. In Figure 4(c), the birefringence narrows more, retaining its diffuse nature only at the low-strain nodes between breaks. No further breaks have occurred, indicating that the strain at which the fiber breaks apart into critical lengths has been exceeded. In Figure 4(d), the sample is approaching failure. The birefringence has become very narrow, and in places where the fiber has slipped, there are long stretches of low birefringence where the strain has relaxed. An asymmetry has also formed in the birefringence slightly to the right of the break indicated by the left arrow. The formation of this asymmetry at deformations close to matrix failure has been suggested by Drzal[9] to be due to shear banding type failure of the matrix induced locally by the fiber.

Figure 5 shows a different area of the same sample after failure has allowed the stress to relax. Arrow a indicates a region where the fiber slipped while in tension, causing a kink in the fiber where the ends compress after meeting during relaxation. Arrow b indicates a more normal birefringence pattern occurring at fiber breaks. The asymmetric shadow indicated by arrow c is a remnant of the matrix failure by such mechanisms as shear banding.

Figure 6 is an optical montage of the birefringence along an uncoated fiber in an E828/1SA matrix under tension. The large amount of asymmetry in the pattern could be due to matrix failure, as before or, as is suggested by the regularity of the distortion, to localized debonding (or, equally, localized adhesion) of the fiber and matrix. Note that the overall pattern is more diffuse than that seen in the coated fiber specimen, indicating a broader area of deformation.

Only limited single-fiber tests were possible in this system. The initial results look promising, but to date, all samples investigated have been formed using a silicone mold release agent. First, the mold release agent might contaminate the fiber surfaces, having an unknown effect on the results, which are

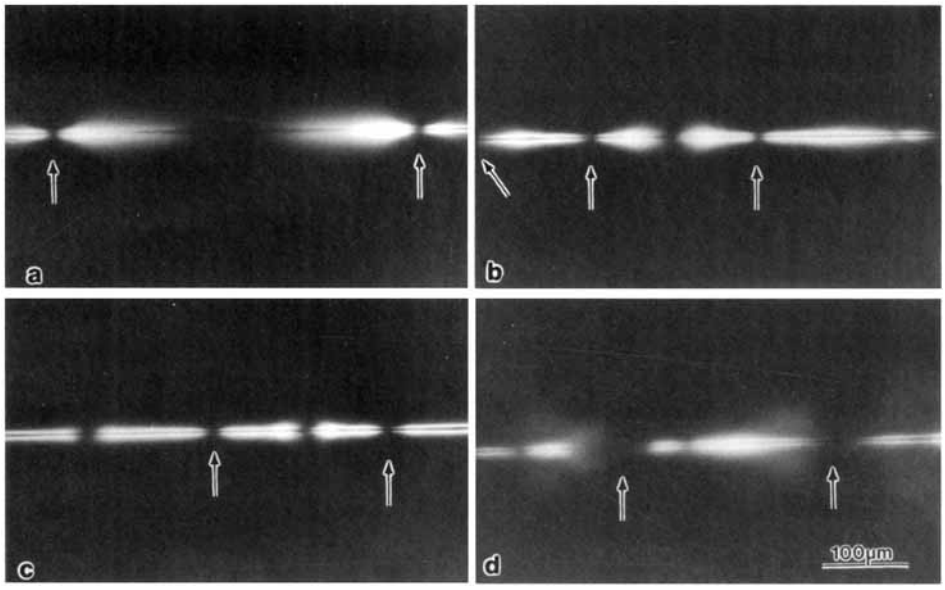

Figure 4 Optical micrographs of the development of the stress birefringence around the coated fiber. (a) Initial fiber breakage: Two breaks are indicated by arrows. (b) Another break has occurred while one break has moved out of the field. (c) The distance between breaks is growing. (d) Final pattern before failure.

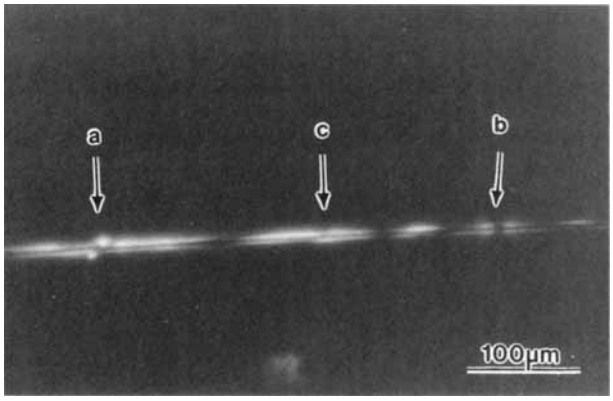

Figure 5 Optical micrograph of the residual birefringence in a coated fiber specimen after failure has allowed the stress to relax. Arrows indicate features of interest. (a) Kink at a fiber break where the fiber slipped under load and then the ends were compressed by sample recovery. (b) Birefringence associated with a normal break. (c) Angled birefringence shadow of unclear origin (see text).

thus in need of confirmation using additional samples. Second, to take full advantage of the single-fiber tests, care must be taken not to greatly exceed the minimum strain necessary to break the fiber apart into its critical lengths. Finally, microtoming along the fiber might be useful in determining whether debonding is occurring or if material adheres to the fiber. These experimental refinements have yet to be performed.

CONCLUSIONS

SEM studies of the unidirectional composite showed that there is excellent adhesion of C8/1SA matrix to fiber and that good load transfer, at least to the rough approximation of the rule of mixtures, enables nearly the maximum obtainable modulus. Aging effects, however, may change this behavior.

The single-fiber tests are interesting, exhibiting many features that are of potential use. The only clear results from the tests, however, were the critical lengths of the uncoated and C8/1SA coated fibers in an E828/1SA matrix. These results suggest that, using C8/1SA as a model, the fluoroepoxies can be successfully employed as fiber coatings with the potential for both preventing the infiltration of moisture along the fibers and improving the interfacial shear strength of materials employing them. Further tests of this nature may be justified.

This research was supported by the Office of Naval Research through the University of Illinois National Center

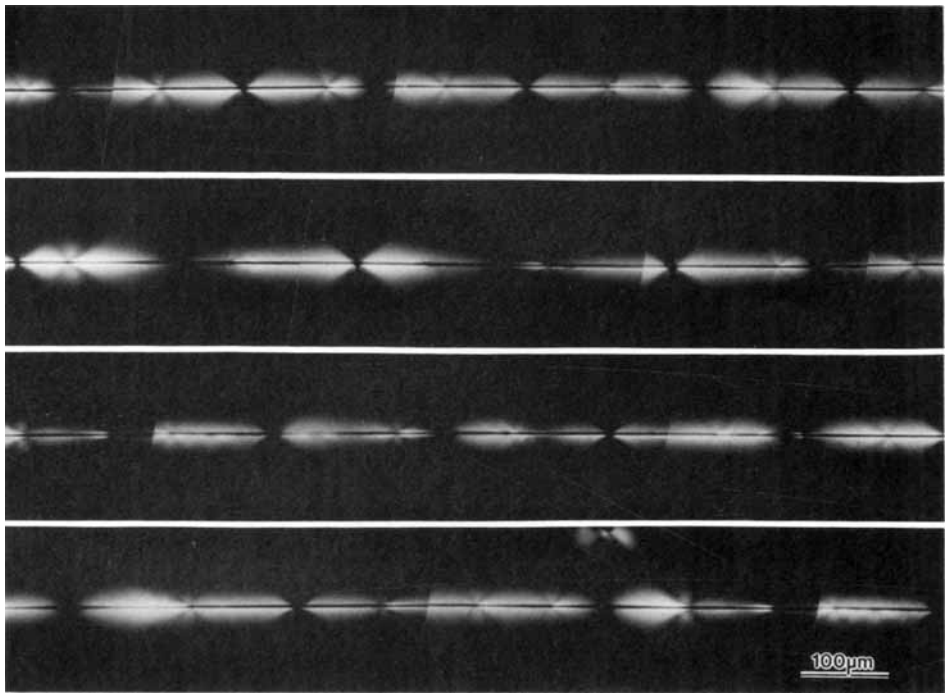

Figure 6 Optical montage along an uncoated AS4 fiber in an E828/1SA matrix illustrating various stress birefringence features (see text). The lighting change from left to right in each photograph is an artifact of the microscope used.

for Composite Material Research. T. E. T. also acknowledges an ONR Fellowship.

REFERENCES

1. D. L. Huston, J. R. Griffith, and R. C. Bowers, *ACS Ind. Eng. Chem. Prod. Res. Dev.*, **17,** 1, 1978.
2. L.-H. Lee, Ed., *Adhesives, Sealents and Coatings for Space and Harsh Environments,* Plenum, New York, 1988, pp. 45–66.
3. J. R. Griffith and D. E. Field, *Report on NRL Progress,* June (1973).
4. J. R. Griffith, *Chemtech,* **12,** 290 (1982).
5. T. E. Twardowski and P. H. Geil, *J. Appl. Polym. Sci.,* **41,** 1047 (1990).
6. T. E. Twardowski and P. H. Geil, *J. Appl. Polym. Sci.,* to appear.
7. L. T. Drzal, M. J. Rich, and P. F. Lloyd, *J. Adhesion,* **16,** 1 (1982).
8. W. D. Bascom and R. M. Jensen, *J. Adhesion,* **19,** 219 (1986).
9. L. T. Drzal, Personal communication (1988).

Received April 16, 1990
Accepted June 19, 1990